Surface Science 83 (1979) 141–161

THE SHAPES OF ISLANDS OF CHEMISORBED ATOMS AS A PROBE OF LONG-RANGE INTERADATOM INTERACTIONS

Theodore L. EINSTEIN

Department of Physics and Astronomy, University of Maryland, College Park, Maryland 20742, USA

Received 27 March 1978; manuscript received in final form 27 November 1978

When ordered superlattices of adatoms are produced by attractive electronic indirect interactions, islands form at low coverages. At low temperatures, the shapes of these domains should bear the mark of these interactions. (For example, at zero temperature a c(2 × 2) island on a square lattice should be square if the second neighbor attraction is at least roughly three times the third neighbor attraction.) First, asymptotic and explicit evaluations of the energies of different configurations are presented. Then some thermal disordering effects are included in a quasicontinuous way. Polygonal-like shapes should be observable at low temperatures, below (possibly much below) 100 K. Complications due to three-adatom interactions can arise in model calculations. Island shapes should be observable using LEED; the adlayer-induced spots should exhibit star-like patterns. Problems such as diffusion and heterogeneity limit the size of islands, making this a problem of metastability. The (111) faces of fcc crystals most likely are the best substrate on which to seek polygonal (i.e., hexagonal) shapes. In any case these ideas provide another aspect by which to compare Monte Carlo simulations with experimental observations.

1. Introduction

In most chemisorption systems the adsorption energy depends strongly on the (lateral) position of the adatom with respect to the surface net. Consequently, the statistical mechanisms of the adatoms are well-described by a two-dimensional lattice gas: The adatoms are localized on a net of sites having the same (or a closely related) symmetry as the surface net, and they occasionally thermally hop from one well to a nearby vacant one. The well depths are modulated by interactions with adatoms in nearby wells, providing the energy parameters of the lattice gas Hamiltonian. The small ratio of these interactions to the single-adatom binding energies distinguishes this problem from physisorption, where the interadatom forces are comparable to the adatom–substrate forces and so the adatoms can move easily out of registry or even desorb. In our problem, at the temperatures at which the intersite interactions play a significant role, desorption is negligible, so that (in the

absence of absorption into the bulk) the adatom number is constant and system essentially two-dimensional.

To the extent that this picture is valid, as it seems to be for transition metal substrates, one can separate out the interadatom interactions from the stronger background effects. Theoretical analyses of model covalently-adsorbed systems have yielded a good qualitative and semi-quantitative understanding of these interactions [1–6]. They are primarily electronic, indirect (i.e., via the substrate wavefunctions rather than due to direct overlap of adatom orbitals), and pairwise. They oscillate in sign as a function of interadatom distance R, decrease rapidly with increasing R, and are strongly anisotropic[7]. Quantitative progress has been hindered by the low symmetry of the problem [1].

Experimental investigations of adatom pair interactions have followed two principal routes. With field ion microscopy (FIM), one can follow the evolution of two adatoms on a plane of a tip [8]. If the adatoms are not limited to one-dimensional motion by use of grooved surfaces, the statistical analysis becomes too complicated to extract anything but qualitative trends [9]. The second approach focuses on the order–disorder transition of adatom superlattices, as monitored by the adlayer-induced, "extra", LEED spots. Estimates of the strongest interactions can be obtained by fitting the [extrapolated] critical temperature T_c at which these spots vanish [4,10]. More information is potentially obtainable by fitting plots of the intensity of the extra spots versus temperature to predications based on Monte Carlo simulations, in which a pre-chosen set of interactions are variable parameters [11,12].

At low coverages, when attractive interactions exist, islands of the ordered adlayer phase may form. The size of such islands can be monitored via the width of the extra spots [13,14]. Although thermodynamics says that equilibrium is a giant condensed domain surrounded by a low-density gas [15], experimental measurements of the widths of the extra spots for p(2 × 1)O/W(110) show that the diameters of such islands are smaller than the LEED beam transfer width even at temperatures well below the disordering temperature [14]. The small size of the islands, although not fully understood, is attributed to diffusion-time limitations or to surface heterogeneity.

The object of this paper is to explore how the *shape* of these islands contains additional information about the adatom interactions – especially some longer-range ones that are usually masked by stronger near-neighbor effects – and to discuss the effects of these shapes on the adlayer-induced LEED spots. To best illustrate our ideas we restrict the discussion to high symmetry faces (mostly square nets, with some generalizations to triangular ones) to minimize the number of parameters W_n needed to describe the system, where W_n denotes the interaction energy between pairs of adatoms at nth nearest neighbor sites. We take for granted that the adatoms have evolved from random adsorption sites to condensed ordered islands with a dilute surrounding "gas". Adatoms in the interior of the island are essentially immobile. Well below the transition temperature those at the edge are

far more likely to migrate around the perimeter than to separate from the island. Conversely, if the system has evolved adequately, the inter-island gas will be so dilute that the accretion rate will be smaller than the diffusion about the perimeter. The central problem we discuss is: Given an island of fixed size, what shape does it take to minimize its free energy? Thus, we contend with questions of equilibrium for each island rather than the whole system, i.e., with metastability.

In section 2 we consider the energetics of different shapes, i.e. the zero-temperature problem. For the square lattice, we consider islands of c(2 X 2) structure produced by a negative W_2. Were there no other interactions, the island shape which minimizes the number of broken bonds would be a square (rotated 45° with respect to the substrate) rather than a circle or octagon. If W_3 is also attractive and greater in magnitude than roughly one-third W_2, then the circle has lower energy. Thus even though W_3 may play a relatively minor role in the thermal disordering of the adlayer, it should be very important in determining island shape. On triangular faces, islands should be hexagonal. Section 3 adds the effect of temperature in a quasicontinuous way. We find that the island shapes blur at temperatures an order of magnitude smaller than the transition temperature, in accordance with the smaller energies involved. Thus, the LEED experiment must be done at very low temperatures (probably below 77 K). Section 4 mentions a possible complication due to three-adatom non-pairwise (trio) energies. The strongest trio interaction sometimes may be comparable to W_3. Section 5 considers the effect of non-circular islands on adlayer-induced LEED spots. Under model circumstances these spots should have a four-lobe star appearance for a square substrate at the very low temperatures mentioned above. We discuss complications, e.g., slow diffusion, which makes this effect difficult to produce in real systems. As noted by Herring in connection with crystal growth [16], for a very large island the effect of our ideas may be the formation of large steps in an unfavorably-oriented edge rather than the evolution of a square. For small islands, this concept of limited movement of adatoms has the implication that individual islands may well lack the full symmetry of the substrate, e.g. by having rectangular-like rather than square-like shapes. For an ensemble of islands these idiosyncrasies tend to average out.

The ideas in this paper are timely and important for the following reasons: (1) LEED equipment and experimentation have reached the sophistication at which island shapes can be explored. (2) Even if not measurable, these ideas provide a helpful conceptualization of what island shapes might be expected to form for given interactions and temperature. We cite in particular a report in the literature of square c(2 X 2) islands with the wrong orientation and at a ridiculously high temperature. (3) From the theoretical side, Monte Carlo simulations are now being applied to the two-dimensional adlayer problem. Characterization of island shapes in the framework to be discussed can and should be extracted from such studies.

2. Zero temperature island shapes

To describe the properties of a c(2 × 2) overlayer on a square surface lattice for coverages less than 1/2, we need at least the *three* nearest pair interaction energies, W_1, W_2, and W_3. (These W's will refer to the bonds themselves as well as their respective energies.) Use of only a strong positive (repulsive) W_1 is adequate for a half monolayer, but fails to give any mechanism for island formation at lower coverages, as Doyen et al. [11] have demonstrated graphically in Monte Carlo computations. We emphasize that the island shape is a sensitive function of the relative strenghts of W_2 and W_3, since these energies determine the boundary energy as a function of orientation. In this section we discuss energetics by counting bonds.

Fig. 1 illustrates a small c(2 × 2) island. For sufficiently large and positive W_1, we can view the substrate locally as a checkerboard with only one "color" of squares occupied; these squares themselves form a square lattice with lattice constant $\sqrt{2}$ times that of the substrate and with axes (indicated by arrows) rotated by 45°. All subsequent discussions will be phrased in terms of this rotated square superlattice.

In the interior of a c(2 × 2) island there are two W_2 and two W_3 bonds per adatom. We know immediately: (1) $W_2 < 0$ to provide a c(2 × 2) overlayer; (2) $W_3 > W_2$ to make c(2 × 2) more favorable than (2 × 2) as the low-coverage phase; and (3) $W_3 < |W_2|$ to prevent simple horizontal and vertical lines (i.e., diagonal lines with respect to the substrate's natural axes) from being the lowest energy arrangement. If W_3 were negligible, then the stable configuration of n^2 adatoms (n being any integer) would be a square [17]. For W_3 comparable to W_2, the surface energy should be roughly isotropic, favoring a more nearly circular domain as the minimum perimeter configuration.

For an $n \times n$ square, inspection shows there are $2n(n-1)$ W_2 bonds (i.e. $2n$

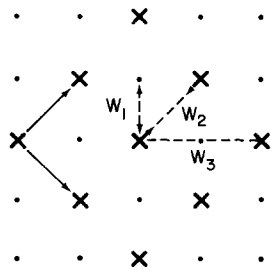

Fig. 1. Sketch showing (dashed lines) the three pair interactions considered for c(2 × 2) islands of adatoms (×) on square lattices of adsorption sites (vacant sites indicated by dots). W_1 is repulsive and W_2 attractive; the sign and size of W_3 determines the energetically-favorable island shape. Also indicated are the natural primitive axes (solid arrows) for the adlayer, which forms a square lattice rotated 45° from the substrate.

missing) and $2(n-1)^2$ W_3 bonds (i.e. $4n-2$ missing). The perimeter contains $4n-4$ adatoms, each of which (except at the corner) is lacking a W_2 and two W_3 bonds.

Islands are often imagined as circles, for which no simple expressions exist for the number of bonds [8]. Explicit computer solutions, to which we turn shortly, are needed to give solutions for the smaller islands of interest; but the asymptotic quasicontinuous case, in which we work to order n, shows the essence: A circle containing n^2 points has a circumference $2n\sqrt{\pi}$. Consider bonds between sites separated by some characteristic distance d. For our superlattice, d is 1 and $\sqrt{2}$ for W_2 and W_3 bonds, respectively. The number of missing bonds is $4nd/\sqrt{\pi}$, to order n [19]. Thus there are roughly $2.257n$ and $3.192n$ missing W_2 and W_3 bonds, respectively. Hence, while a square has a longer perimeter and more missing W_3 bonds than a circle, it has fewer missing W_2 bonds due to the favorable orientation of its flat sides. For W_3 repulsive or weakly attractive, a square will have lower energy than a circle of equal area. The minimum ratio of W_3 to W_2 in order for circles to be favored is $[(4/\sqrt{\pi})-2]/[4-4\sqrt{(2/\pi)}]$ or 0.3176. Exact calculations reported below show that the asymptotic value is reached ±3% for $n \geqslant 229$.

Readers acquainted with Wulff's theorem [20] for equilibrium crystal shape – which states that the distance of faces from the crystal center are proportional to their surface free energy per unit area [16,21,22] – will recognize that a circle is the energy minimum configuration only for an isotropic interadatom (attractive) force. For just W_2 and W_3 bonds, the equilibrium shape is an octagon with 4 mm symmetry (an equiangular octagon with the diagonal sides not necessarily equal to the horizontal and vertical ones). The edge energies per unit length in the ⟨10⟩ and ⟨11⟩ superlattice directions, $U_{\langle 10\rangle}$ and $U_{\langle 11\rangle}$, are $-(\frac{1}{2}W_2 + W_3)$ and $-(\frac{1}{2}W_3 + W_2)/\sqrt{2}$, respectively. (Recall $W_2 < 0$.) The ratio of the length of a diagonal side to that of a horizontal or vertical side is $(\sqrt{2}\,U_{\langle 10\rangle} - U_{\langle 11\rangle})/(\sqrt{2}\,U_{\langle 11\rangle} - U_{\langle 10\rangle}) = 3W_3/[(W_2 - W_3)\sqrt{2}]$. For $W_3 = 0$, this ratio vanishes, indicating the octagon reduces to a square as expected. A regular octagon (i.e. ratio unity) obtains for a ratio W_3/W_2 of 0.3204 ..., almost the same as the value for which the circle has the same energy as the square [23]. When temperature is included, much of the octagonal shape will get washed out, so we shall not dwell further on this option.

For smaller islands effects of order unity come into play. An exact expression was given above for squares. Note that a corner site has energy $-W_2 - \frac{3}{2}W_3$, i.e., $-\frac{1}{2}(W_2 + W_3)$ greater than the energy per edge site.

To study circular domains we require explicit (computer) enumeration [24]. For simplicity, we consider only arrangements with an adatom at the origin of the circle, so that the number of sites enclosed by a circle is an integer that is one modulo four. Table 1 displays results for all $n < 100$ which satisfy both the square and circle criteria. For very small islands there is little ($n < 10$) or no ($n < 6$) difference between squares and circles. For all but the degenerate cases, the square again has more W_2 bonds and fewer W_3 bonds than the circle. The W_2 bond number

Table 1
For a c(2 × 2) superlattice, compilation of the number of missing W_2 and W_3 bonds for $n \times n$ square islands and each corresponding circular island containing n_2 adatoms (these circular domains have an adatom site at their origin); the total number of each kind of bond is just twice the number of adatoms minus the number of missing bonds; the column labeled ratio gives (column 4 − column 3)/(column 5 − column 6), which is the ratio of W_3/W_2 above which the square has lower energy

n	Adatoms	Missing W_2 bonds		Missing W_3 bonds		Ratio
		Square	Circle	Square	Circle	
3	9	6	6	10	10	–
5	25	10	10	18	18	–
7	49	14	18	26	22	1.00
9	81	18	22	34	30	1.00
11	121	22	26	42	34	0.50
13	169	26	30	50	42	0.50
15	225	30	34	58	50	0.50
21	141	42	50	82	66	0.50
23	529	46	54	90	74	0.50
35	1225	70	78	138	110	0.29
37	1369	74	82	146	118	0.29
45	2025	90	102	178	142	0.33
47	2209	94	106	186	150	0.33
51	2601	102	114	202	162	0.30
53	2809	106	118	210	170	0.30
55	3025	110	126	218	174	0.36
57	3249	114	130	226	180	0.36
61	3721	122	138	242	194	0.33
63	3969	126	142	250	202	0.33
71	5041	142	162	282	226	0.36
73	5329	146	166	290	234	0.36

difference divided by the W_3 difference is tabulated in the column marked "ratio". This ratio gives the critical value of W_3/W_2 below which squares have lower energy than circles. Note that for small islands this ratio is larger than the asymptotic value, indicating an increased tendency toward square shape for given W_2 and W_3. The conclusion for c(2 × 2) islands is that if W_3 is positive or if its magnitude is less than roughly a third to a half of $|W_2|$, then the stable domain shape will be a square. Otherwise it will tend toward circular.

While the preceding discussion was couched in terms of the physically-interesting case of a c(2 × 2) adlayer, it actually applies to *any* square superlattice structure, viz. (1 × 1), c(2 × 2), and (2 × 2), lower density patterns being unlikely due to the rapid decay of the pair interaction with separation. In the (1 × 1) case, the W_3–W_2 competition detailed above translates to a W_2–W_1 competition; in the (2 × 2) case,

it is a W_5–W_3 competition; in all three cases, the ratio of the relevant pair separations is $\sqrt{2}$.

This whole approach generalizes readily to a hexagonal face. If the first attractive pair is W_1, W_2, or W_3, the adlayer pattern is (1×1), $(\sqrt{3} \times \sqrt{3})R30°$, or (2×2), with saturation coverages of 1, 1/3, and 1/4, respectively [25]. For purposes of estimating island shape, the interaction between pairs closer than the first attractive diad (W_1 for $(\sqrt{3} \times \sqrt{3})R30°$, W_1 and W_2 for (2×2)) are viewed as infinitely repulsive. If the attractive interaction is the only active finite force, then the islands at presaturated coverages should assume a hexagonal shape. At $T = 0$, one can again view the shape problem as a competition between the first attractive pair and the next-farther-separated pair in the adlayer (that is not forbidden by one of the repulsions). In the three cases cited, these pairs are W_2, W_5, and W_6, respectively, in each case representing a separation that is $\sqrt{3}$ as great as that of the first attractive pair. Thus the ratio of this second interaction to the first attractive interaction should be considerably smaller than on a square lattice because of the rapid decay of the pair interaction [26]. This aspect strongly favors the hexagonal shape over a circular (or dodecagonal) one; it far outweighs the result that the critical ratio of competing bond energies is here 0.2763 asymptotically versus 0.3176 for the square [27].

3. Finite-temperature results

At non-zero temperatures, entropy factors will complicate the problem of finding the metastable shape of the islands. In essence, as Herring noted [16], polygons require straight edge sides, in effect a one-dimensional ordering, which is impossible at finite temperature. On the other hand, very low temperature should not create much observable difference. Here temperature rounds off sharp corners and bows out straight sides [28].

The details of the thermal evolution of small islands require extensive Monte Carlo simulations. We consider just the quasicontinuous case most appropriate for large islands, with the implication that as in the zero-temperature case the smaller-size results will be similar. In particular, we use the results derived by Burton, Cabrera, and Frank [21] (hereafter BCF) in their classic study of crystal growth. BCF find the local mean direction of the edge of a single-layer nucleus under the assumption that certain configurations (called overhangs) contribute negligibly. The quasicontinuous limit is needed to be able to integrate a differential equation for the nucleus boundary.

In the case of vanishing W_3, and very repulsive W_1 as above, the perimeter is given by

$$2|y/u| = 1 + \beta^{-1} \ln\{1 - [\sinh(\beta x/u)/\sinh(\beta/2)]^2\} , \tag{1}$$

where β is $-W_2/2k_BT$, the x–y axes are in the $\langle 10 \rangle$ directions of the superlattice,

and the origin (unlike in BCF) is at the center of the island. At $x = 0$, y is $\pm u/2$, indicating a figure with "diameter" u in the ⟨10⟩ directions. The logarithm diverges at $x = \pm u/2$, pointing out the need to include "overhangs" when $|y'(x)/u|$ is greater than one. For the square one can surmount this problem by taking advantage of the four-fold symmetry and plotting eq. (1) only for $|y| > |x|$. In the right and left quadrants one interchanges x and y in eq. (1). Ideally one would want $|y'(x)/u|$ to be unity at $|y| = |x|$ in order for the derivatives to join smoothly. While this does not occur precisely, the error is less than 10% (usually much less) for the curves of interest, so that there was never a problem in graphing. As BCF note, the radius of curvature at the corner is $(-\sqrt{2}\, u/\beta) \tanh^2\beta$.

Fig. 2 shows metastable island shapes for $\beta = 2, 3, 4$, and 5. For reference we have included a square with side u and circle with diameter u. As $T \to 0$ ($\beta \to \infty$), the curves look nearly square. For smaller β, remnants of the square shape wash out so that by $\beta = 2$ the plot is scarcely distinguishable from a circle. For β still smaller, the analysis collapses. Although the plots are presented for constant u to emphasize the destabilization of the straight square sides, in a real system u increases with decreasing β so that the perimeter enclosed a constant area.

The temperatures in question are quite low, not at all near the melting tempera-

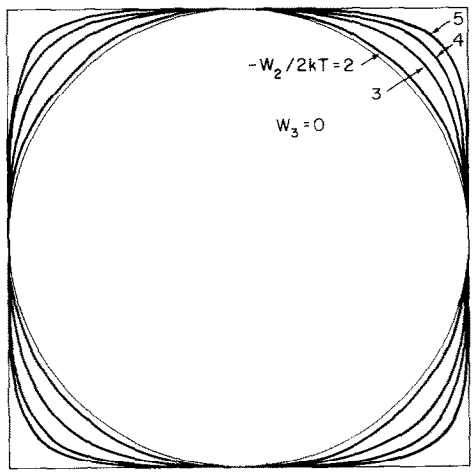

Fig. 2. Shape of c(2 × 2) islands as a function of temperature, for the special case $W_3 = 0$, using eq. (1). The picture assumes no nearest neighbor occupation $W_1 \gg |W_2|$) and a moderately large island. At zero temperature, the stable island shape is square (light line), with sides along the substrate ⟨11⟩ directions (i.e., the ⟨10⟩ axes of the adlayer when viewed as a square lattice). As temperature rises, the sides bow out (if we had normalized area) and the corners round off. The plots are $-W_2/2kT = 5$, 4, 3, and 2, moving toward the center. The analysis collapses when (or before) the plot resembles a circle (light curve) i.e., a ratio of 1.5 to 1. (Reprinted with permission from CRC Critical Reviews in Solid State and Materials Sciences [1]. Copyright the Chemical Rubber Co., CRC Press, Inc.)

ture. Typically in model calculations [4,5], $-W_2$ is of order 0.01 to 0.03 in units of one-sixth the bandwidth, i.e., roughly 10 to 60 meV for transition metals, or equivalently 100 to 700 K. The smallest β for which one could see square-like structure seems to be about 4, implying temperatures in the range 15 to 88 K, most of which lie below the liquid nitrogen boiling point. An alternate approach uses the order–disorder temperature for the c(2 × 2) pattern itself [4]. Since the c(2 × 2) pattern for a half monolayer is equivalent to an antiferromagnetic Ising model with second neighbor ferromagnetic coupling ($W_2 < 0$), and with zero external field, we invoke [4] the very good approximate solution [29],

$$\beta_c = (|W_2|/W_1) \ln[\exp(-2\beta_c) + \sqrt{2}\exp(-\beta_c)] , \tag{2}$$

where $\beta_c \equiv |W_2|/2kT_c$. Table 2 presents sample evaluations of this formula over the physical range of $W_1/|W_2|$. Thus, if this ratio lies between 2 and 8, a β of 4 corresponds to a temperature of 1/15 to 1/43 the order–disorder temperature of a saturated superlattice; taking 600 K as a typical value, we find this β indicates a temperature in the range 15–40 K.

In allowing for non-vanishing W_3, it is natural to introduce a new parameter $\tilde{\beta} \equiv -(W_2 + 2W_3)/2kT$. Then after much algebra the expression presented by BCF can be written

$$2|y/u| = 1 + \tilde{\beta}^{-1}\left\{\ln\{1 - [\sinh(\tilde{\beta}x/u)/\sinh(\tilde{\beta}/2)]^2\} - \ln\left[\frac{1 + f(\beta,\tilde{\beta})\cosh(2\tilde{\beta}x/u)}{1 + f(\beta,\tilde{\beta})}\right]\right\},$$

$$f(\beta,\tilde{\beta}) = (e^{\tilde{\beta}} - e^{\beta})/(e^{\beta}\cosh\tilde{\beta} - 1) . \tag{3}$$

In fig. 3a we fix β at 4 and plot a quadrant of an island for W_3/W_2 being 1/2, 0, and $-\frac{1}{4}$. The quite repulsive W_3 scarcely stabilizes the square, and even for a

Table 2
Values of the order–disorder temperature for an antiferromagnetic second-neighbor square Ising model, using eq. (2); the final column gives the ratio T/T_c when $\beta \equiv -W_2/2kT$ is 4, roughly the lowest β at which square islands are easily visible

$W_1/\|W_2\|$	W_1/kT_c	$-W_2/kT_c$	$T(\beta = 4)/T_c$
1	0.744	0.744	0.093
2	1.042	0.521	0.065
3	1.205	0.402	0.050
4	1.307	0.327	0.041
5	1.378	0.276	0.034
6	1.429	0.238	0.030
7	1.469	0.210	0.026
8	1.500	0.187	0.023
9	1.525	0.169	0.021

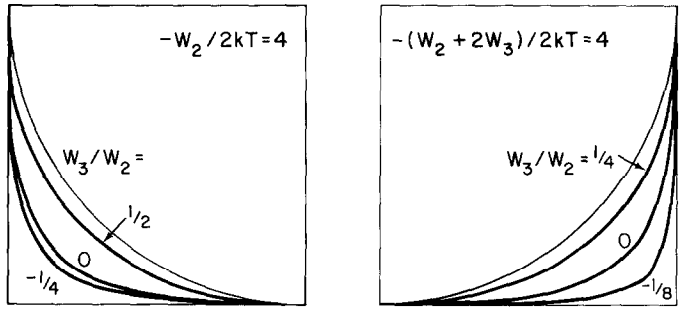

Fig. 3. Quadrants of a plot equivalent to fig. 1 for the general case of W_3 finite. A light curve again gives the limit of the circle. (a) In the left panel, $-W_2/2kT$ is fixed at 4. Moving inward (up and right) the curves give the result of eq. (3) for $W_3/W_2 = -1/4$, 0 and 1/2. In contrast to the zero-temperature view of section 2 and table 1, a strongly attractive W_3 (ratio 1/2) does not completely destabilize the square, and a repulsive W_3 does not stabilize it much. (b) Fixing $-(W_2 + 2W_3)/2kT$ at 4, we plot eq. (3) for $W_3/W_2 = -1/8$, 0 and 1/4, moving inward (up and left) and find behavior similar to that at zero temperature. The physical idea is that temperature destabilizes the flat sides of a square so that the relevant energy to compare with temperature is the edge energy per unit length.

very attractive W_3 we are far from circular. This behavior is strikingly different from the $T = 0$ results. To retrieve the zero temperature behavior the dimensionless parameter $\tilde{\beta}$ rather than β must be fixed as W_3/W_2 is varied. The principal effect of temperature is destabilization of the $\langle 10 \rangle$ straight edge; hence T should be related to $U_{\langle 10 \rangle} = -(1/2\, W_2 + W_3)$. In fig. 3b, then, $\tilde{\beta} = 4$ and W_3/W_2 takes on values $-1/8$, 0, 1/4. A small repulsive W_3 promotes square-like shape. For $W_3/W_2 = 1/4$, the curve is pushed somewhat toward circular; for $W_3/W_2 = 1/2$ the curve would be scarcely distinguishable from circular. As for $T = 0$ the circularity occurs for $W_3/W_2 \gtrsim 1/3$. (Recall, however, that W_3/W_2 is fixed for any one system: only T is readily varied.)

In the (2 X 2) hexagonal case, the physics should not be too different. Temperature will now destabilize the flat edges of the hexagon, the energy per spacing of which is $U_{\langle 100 \rangle} = -W_3 - \frac{3}{2}W_6$; W_6, however, is usually negligible. If W_3 for a (111) face were similar to W_2 ($+2W_3$) for a (100) face of a cubic crystal, then β, and hence the shape disordering temperature for the triangular face, would be (roughly) twice that for the square face. Unfortunately, no systematic calculations of pair interactions on hexagonal faces have been reported [30]. The only analogue to eq. (2) are two results for $(\sqrt{3} \times \sqrt{3})R30°$ adlayers, i.e., antiferromagnetic triangular Ising models with ferromagnetic second-neighbor coupling. In the Bethe–Peierls approximation (which overestimates T_c) and for $W_1 = 5|W_2|$, $|W_2|/kT_c \geqslant 0.343$ ... [31]; in a Monte Carlo scheme for $W_1 = |W_2|$, $|W_2|/kT_c \geqslant 0.685$ ... [32]; in both cases, the equality holds for $\theta = 1/3$. These saturation-coverage values compare reasonably with those in table 2. We expect the dimensionless transition temperature to be

higher than for the c(2 X 2) case, since it increases with the number of nearest neighbors [33].

The upshot of this discussion is that on triangular faces, the temperature at which polygonal shapes are obscured can be reasonably taken at roughly an order of magnitude smaller than T_c; Monte Carlo calculations are needed to refine this estimate [34].

4. Three-adatom effects

Before considering experimental consequences of the preceding discussion, we mention a possible theoretical complication which may sometimes cloud the picture. We have verified recently [1,35] that the W_2 bond dominates the interaction energy per adatom in a full c(2 X 2) layer on a square face, with the sum over pair bonds converging well. However, trio effects – the non-pairwise interaction energies of three adatoms – were found to be more substantial than expected. These trio energies themselves form a subhierarchy which tend to decrease in strength as the two shortest legs of the triangle formed by the three adatoms increases. In particular, for a c(2 X 2) adlayer, there are two types of trios containing two W_2 bonds: One has these two at right angles with a W_3 bond completing the triangle, the other has the two W_2 bonds colinear (with a fifth nearest neighbor bond completing the triangle).

For comparison with previous work [1,4,35], we have calculated the relevant energies using for a substrate the (100) face of a semi-infinite single band tight-binding crystal with a diagonal energy at the energy zero (implying the bond centered about the energy origin) and with nearest neighbor hopping of $-1/2$ (implying a bandwidth W_b of 6 in these unspecified energy units). The adatoms are represented by a single level E_a (here taken at 0.3 below the band center) which includes Coulomb effects in some Hartree–Fock sense. For simplicity and definiteness, the adatoms are in the atop position, and couple with a hopping parameter $-V$ (here $-3/2$) to the nearest substrate site. Self-consistency and correlation effects are not explicitly included, but are even less important for this problem than for the two-adatom interaction [36]. If the adatoms sit above sites, 1, 2, and 3, then their total indirect interaction energy is

$$W_{123} = -\frac{2}{\pi}\int_{-\infty}^{E_F} dE \tan^{-1}\left[1 - \frac{V^4(G_{12}^2 + G_{23}^2 + G_{13}^2)}{(E - E_a - V^2G_{11})^2} - \frac{2V^6G_{12}G_{23}G_{13}}{(E - E_a - V^2G_{11})^3}\right], \quad (4)$$

where the G's are energy dependent Green's functions for sites on the surface. The pair interaction between say the adatoms at sites 1 and 2, W_{12}, can be obtained from eq. (4) by setting G_{23} and G_{13} to zero. The trio interaction is defined as $W_{123} - W_{12} - W_{13} - W_{23}$.

Fig. 4 gives the results of these calculations, with the various interaction energies

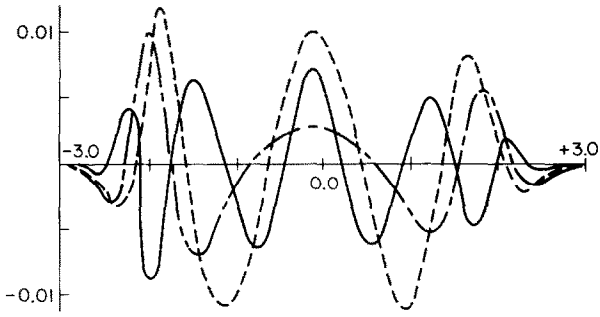

Fig. 4. Plots of relevant interaction energies vs substrate Fermi energy in units of one-sixth bandwidth. Adatoms are atop surface atoms of a (100) simple cubic crystal, with an energy slightly below the middle of the substrate coupling ($V = 3/2$). The dashed curve gives *one-third* the second neighbor indirect interaction W_2. Presuming W_1 repulsive, the c(2 × 2) superlattice will in this model exist for $W_2 < 0$, i.e. $|E_F \pm 1| \leq 0.5$. The third neighbor interaction W_3 is given by the dash-solid curve. The curves are of comparable magnitude. Square c(2 × 2) islands are predicted when W_3 curve does not lie below $W_2/3$, in this example everywhere in the previous range except for $E_F \sim \pm 1.5$. The solid curve gives the trio (three-adatom non-pairwise interaction for a right triangle if adatoms (2 W_2 pairing, 1 W_3 pairing). It is comparable to W_3 here, and may complicate the analysis. (Reprinted with permission from CRC Critical Reviews in Solid State and Materials Sciences [1]. Copyright The Chemical Rubber Co., CRC Press, Inc.)

plotted versus the Fermi energy (i.e., going from an empty band on the left to a filled band on the right). Since an attractive W_2 bond is a prerequisite for c(2 × 2) adlayer structure, in this *particular* case we would find a c(2 × 2) pattern for substrate bands which are roughly 1/3 or 2/3 filled (i.e., $E_F = \pm(1.0 \pm 0.5)\, W_b/6$) or possibly nearly empty or filled (although in these cases W_2 is rather weak and also there would be sufficient charge transfer to make the calculation questionable); these details depend to various degrees on adatom binding site, E_a, and V in our model, and in real systems on the exact shape of the substrate bands.

The magnitude of W_2 is typically three to four times that of W_3. For clarity we have plotted *one-third* of W_2 (for which the dashed form should serve as a reminder). On this plot when the W_3 curve lies near or below the $W_2/3$ curve, we would expect the islands to tend to circular; E_F near −1.4 or +1.2 would be such places. For E_F in the ranges −1.0 to −0.5 and 0.5 to 1.0, fig. 4 suggests square-like domains should exist for this particular case. The solid curve gives the trio interaction energy for the right isosceles W_2–W_2–W_3 triangle. Its magnitude is comparable to that of W_3, which may at times complicate the analysis. Hopefully this paper will stimulate calculations of pair and trio interactions in more realistic systems to permit more quantitative statements.

5. LEED ramifications and general discussion

Experimentally, the island shapes explored above should be observable in LEED. In essence, this is the problem of Fraunhofer diffraction from an aperture of given shape except that we now have a discrete (but dense) set of scatterers rather than a continuous one. For an mxn rectangle with lattice constant d, the summation of a geometric series gives the familiar expression [37]

$$I = I_0 \frac{\sin^2(mK_x d/2)}{\sin^2(K_x d/2)} \frac{\sin^2(nK_y d/2)}{\sin^2(K_y d/2)}, \tag{5}$$

where $\boldsymbol{K} = \boldsymbol{k}' - \boldsymbol{k}$ is the elastic scattering vector. The result [38] is a bright central maximum of size $2\pi/md$ by $2\pi/nd$ with subsidiary maxima in the ⟨10⟩ directions in K space and weaker replica maxima off these axes. For a square ($m = n$), the pattern has 4mm symmetry. Along say the x axis, the pth subsidiary maximum is centered at $K_x d/2 = \pi(p + 1/2)/m$, at which its intensity is

$$\{m \sin[\pi(p + 1/2)/m]\}^{-2} = [\pi(p + 1/2)]^{-2}[1 + O(p/m)]$$

times that at $\boldsymbol{K} = 0$; i.e. for islands large enough so that the discussion of shape is meaningful, the first three subsidiary maximum intensities are 5%, 2%, and 1%, respectively, of the peak at the "origin".

In a real situation there will be a variety of domain sizes; the nodes between subsidiary maxima will wash out, leaving a four-fold star pattern as indicated schematically in fig. 5. The lobes will be oriented along the ⟨10⟩ axes of the *adlayer*, indicated in fig. 1. When only a few well-separated islands lie within the coherent window [39], such stars exist in principle on *all* LEED spots, but generally will be observable only on the extra spots [40].

The resulting LEED screen intensity pattern can be straightforwardly stimulated with a computer [41]. Naturally, finite temperature will blur this simple picture. For islands with bowed-out sides but with sharp corners the star lobes flare out like a Maltese cross (with rounded tips), so that the envelope lines up with a tangent to the bulging square near the far corner [42]. The intensity within the lobes will correspondingly be reduced. The rounded corners will further lower intensity within the lobes, scattering it into the background. These remarks have also been confirmed in our computer stimulation. For a (2 X 2) island on a hexagonal substrate the star naturally will have six lobes; otherwise the physics is similar.

The shape and the size of the LEED spots from commensurate overlayers are not significantly influenced by the many complications which plague the analysis of intensity versus energy (e.g. atomic scattering factors, multiple scattering effects, Debye–Waller factors [43]). The instrument response limits the effective coherent width of the LEED beam; this restriction can be taken into account by convoluting the intensity with a transfer function [14,44]. From the theorist's viewpoint, especially when dealing with Monte Carlo simulations, it is more convenient to account for the instrument limitation by saying that the measured data come from

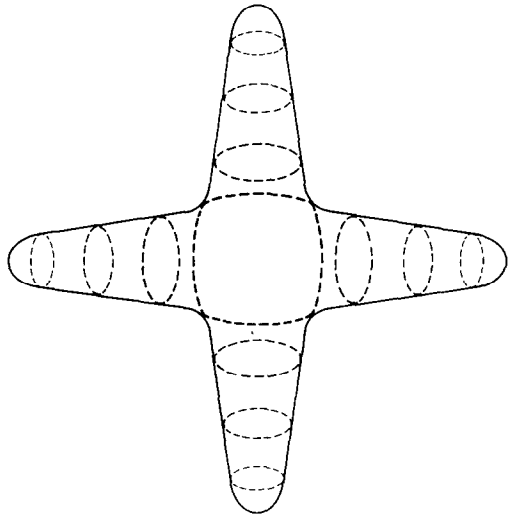

Fig. 5. Schematic of an adlayer-induced LEED spot shape from square domains. The area enclosed by dashed lines indicates the bright areas in the diffraction pattern from a square aperture [38]. Interference between islands of different sizes will fill in the gaps to give the star enclosed by the solid lines. The lobes will point along the axes of the square islands producing the pattern. Finite temperature effects will flare out the lobes and generally diffuse the intensity, but contours of constant intensity will still exhibit four-fold character. In the limit of circular or random-shaped islands, the intensity becomes fully rotationally symmetric.

the lattice scattering viewed through a [movable] window function. (A precise relationship exists between these two equivalent perspectives: The Fourier transform of the transfer function is the convolution square of the window function [45].) This window function limits the range of the surface over which a LEED measurement can give information; if the island is larger than this range, the LEED beam will not portray its shape clearly. The order of magnitude of the width of this window is typically 100 Å for existing instruments, but the actual number is sensitive to the energy of the beam and its angle of incidence and reflection; it can be increased significantly by going to grazing angles and lower energies, and decreased correspondingly by doing the opposite [44]. Thus, for a polygonal island with mean size in this range, one should be able alternately to obtain and diffuse the star-shaped pattern by adjusting the beam parameters.

In contrast to the enormous effort that has been devoted to obtaining and interpreting complicated LEED intensity profiles, little attention, until recently, has been given to the geometry of the spots. In the nearly-saturated-coverage regime, complementary to the low-coverage case envisioned in this paper, adatom islands abut each other. Depending on the symmetry of the substrate, the resultant interference between domains can lead to splitting [46] or streaking [37] of the adlayer-induced spots. In the low coverage regime, streaks can arise from rows

of adatoms perpendicular to the streak direction. Streaks produced by one-dimensional domains are by their very nature an indication that compact polygonal patches are not the dominant low-coverage adatom arrangement. These linear "islands" can result from (1) pronounced grooves on the surface (e.g. W(211)) or any comparable substrate one-dimensional character; (2) adsorption onto bridge sites or other positions lacking the point symmetry of the substrate, leading to widely differing indirect interactions between pairs with the same or similar separations but with differing orientations relative to the substrate (e.g. in fig. 1 two bridge-bonded adatoms separated by the lattice spacing might or might not bond to the same substrate atom), (3) a strong pair repulsion for two adatoms farther apart than the pair whose attraction produces the periodicity along the linear domain (e.g. as suggested in section 2 for a square substrate, the case $W_1 > 0$, $W_3 > -W_2 > 0$ will produce diagonal rows of adatoms), (4) an anomalously strong, repulsive trio interaction, as implied in section 4.

Recently Lagally and coworkers [13,14,47] drew attention to the store of information in adlayer-induced LEED spots. By carefully probing the size of these spots for O(2 × 1)/W(110) at low coverages, they showed that islands dominate in this regime; thermal disordering comes from "evaporation" of the islands into the background two-dimensional lattice "gas", rather than disordering of a saturated overlayer via occupation of repulsive sites ("Bragg–Williams disorder").

From droplet models of the condensation process [15] the low-temperature equilibrium configuration is a single huge ordered island surrounded by dilute gas. In their investigations, however, Wang et al. [14,48] were unable, within the few hours of an experimental run, to obtain islands larger than roughly 60 Å across (11 oxygen atoms in the alternately occupied direction, 22 in the substrate-periodic direction). As explanations, they suggested surface heterogeneity and diffusion time limitations. The former encompasses the problems of terraces, dislocations, and defects on the clean surface. If present on the scale of say the LEED beam coherent-window, these features will obviously significantly affect surface dynamics more than interadatom interactions, since the characteristic energy of an adatom–heterogeneity interaction is at least that of the diffusion barrier. Resultant shape effects, such as the creation of a flat island side by abutting a terrace, should not show much thermal dependence till much higher temperatures than predicted for interadatom-induced shapes. The observation that island size goes linearly with coverage for low θ [48] is consistent with nucleation about point defects.

The principal role of diffusion is to limit the approach to equilibrium of the random configuration resulting from the initial adsorption. Herring noted [16] that from some given initial shape crystals often will not attain their absolute free energy minimum but rather some metastable shape achievable through movement of a relatively modest number of constituents. Thus, for large islands an energetically unfavorable face (here, an edge) will tend to reform into steps with lower-energy orientations rather than disappearing entirely. Such processes are so complicated that Monte Carlo simulations are necessary (except near T_c) [49] as in

Binder and Stauffer's [50] study of the relationship between island size and boundary length. Preliminary Monte Carlo calculations [51] do show evidence of star-like features in the adlayer spots.

To minimize the diffusion barrier, one should select crystal faces with a high packing fraction. (Such a choice also minimizes the rate of adsorbed atoms passing into the bulk; that this rate be negligible is crucial to having a fixed-coverage two-dimensional system, an implicit assumption here.) If we further demand 4mm or 6mm symmetry to simplify the analysis, we are led to favor fcc and hcp crystals over bcc. Barriers for chemisorbed systems are around 1/4 to 1 eV, substantially less than the binding energy [52], as indicated in our analysis of the lattice gas picture.

The intrinsic problem is that the barrier height must be sufficiently greater than the lateral interactions to validate the lattice gas picture, but not so much greater that no diffusion takes place at the low temperatures at which these interactions influence island shapes. Thus, careful selection of experimental systems and delicate temperature control may be necessary to achieve, within the few hours that the sample stays clean, an observable approximation of the adatom equilibrium configuration.

To optimize the selection of real systems in which to test our ideas, a search of the literature was undertaken [53]. Curiously, there is a report of square islands allegedly observed by Leggett and Armstrong for c(2 X 2) H/W(100) using a crude HEED system [54]. This intriguing result does not represent a realization of our proposed scenario for several reasons: (1) These experiments were performed above room temperature, i.e. over half the saturated c(2 X 2) order–disorder temperature [10], and so much too warm to exhibit indirect-interaction-induced polygonal shapes. (2) The lobes of the 4-fold stars are along the substrate (rather than adlayer) ⟨10⟩ axis, i.e., rotated 45° from where they should be in our picture. (3) The structure persists to saturated coverage and indeed goes through to a domain-interference spot-splitting pattern. (4) Around or below room temperature, reconstruction of the clean (100) faces of W and Mo [55] makes suspect any simple lattice model discussion of adsorption. In fact, Barker and Estrup [56] have just carefully reexamined H/W(100) in light of new data and concluded that at a coverage of 0.3, where our island picture would be applicable, the adsorption actually induces a reconstruction similar to the lower temperature reconstruction of the clean surface. (Their LEED spot shapes and orientations are all consistent with the HEED results just cited.) These exciting new findings make (100) bcc crystals an undesirable class of substrates on which to seek island shapes.

On [100] fcc transition metals, there are [53] c(2 X 2) for the following systems: CO, O, S on Ni; CO, O, N on Cu; CO, O on Rh. In the first four cases, a lower coverage (2 X 2) pattern is also found, indicating that square islands should never be stable. In fact, in all but N on Cu, some lower coverage ordered phase is reported. Of hexagonal faces, the bcc [111] faces are too loosely packed (less than half the packing fraction of [110] faces). For fcc materials, however, [111] faces

are close-packed, as are the [0001] faces of hcp crystals. The $(\sqrt{3} \times \sqrt{3})R30^\circ$ pattern in chemisorption systems is invariably preceded by a (2×2) phase. Examples are O, CO, S on Ni; O, S on Cu; O on Ag; Co on Ir; and CO on Ru. The (2×2) pattern is also found for H on Ni; O, CO on Rh; O, CO on Pt; O on Ru; and O, CO on Re. Only for O/Ni has the temperature dependence been carefully monitored, with an order–disorder transition observed at 160°C [57]. The (2×2) adlayer requires special attention since the associated LEED spot pattern is the same as that produced by threefold degenerate (2×1) domains. By monitoring adlayer-induced spot intensity versus coverage, one can distinguish between these two patterns. If the intensity peaks at $\theta = 1/4$, as happens for O/Ni, [58] the superlattice is (2×2), while if it peaks at $\theta = 1/2$, the structure is (2×1), as for O/Ru. [59] Thus, O/Ni (111) is a propitious system for which to start a search for evidence of hexagonal islands [60].

To summarize, we have discussed how the attractive indirect interactions which produce internally-ordered islands of adatoms at low coverages may also cause these islands to have polygonal-like shapes. Thermal effects are very important, not only in rounding the edges of the island but also in limiting the diffusive approach to equilibrium. Moreover, multi-adatom effects may sometimes complicate matters. Much theoretical work remains to be done, particularly using Monte Carlo simulations. On the experimental side, few systems have been studied with the care required for this search. The procedure is: (1) Check that the lowest coverage stable phase exists at a low enough coverage to show that it does not come just from minimizing repulsive interactions but rather is caused by attractions, and hence has islands; make sure that this regime does not show streaking characteristics of rows of adatoms rather than compact patches. (2) By measuring the temperature and the coverage at which the phase disorders or changes, estimate the relevant lateral interaction strengths. (3) Based on these estimates, determine the zero-temperature equilibrium shape of the islands. If it is square or hexagonal, predict the orientation of the 4 or 6 star lobes and scrutinize the adlayer-induced LEED spots for this behavior. All efforts must be made to optimize diffusion without thermally destroying the island shape. Since the observable spot will probably be highly diffuse, and the star lobes hard to discern visually, this search should take the form of mapping contours of constant intensity. (4) Finally, to refine evaluation of the interaction strengths, repeat the experiment for several different temperatures to gauge how the island loses its polygonal boundary with increasing temperature. The resulting information is important to understanding fully the low coverage regime in which adsorbed species are most active. The degree to which the ideas expressed here are not realized experimentally should give some idea of restraints to the approach to metastability. Island shape is, in short, a useful and accessible feature that offers another check between the predictions of model calculations and the test of experimental observation.

Acknowledgments

This work was supported in part by NSF-DMR 76-82519. The University of Maryland Computer Center supplied computer time and use of its facilities. CRC Press permitted reproduction of two figures.

This work has profited throughout from numerous stimulating and informative discussions with R.L. Park. Frequent conversations with P.I. Cohen (who also critically reviewed the manuscript), A.R. Kortan, L.D. Roelofs, and the members of the University of Maryland solid state theory group were valuable, too. Sincere gratitude goes also to the following: M.G. Lagally and G.-C. Wang who forwarded several manuscripts prior to publication and offered many useful comments. R.A. Barker and P.J. Estrup, and E.D. Williams, S.L. Cunningham, and W.H. Weinberg sent unpublished work. A discussion with M.B. Webb helped clarify some of the experimental complications.

References

[1] T.L. Einstein, invited paper at 3rd Intern. Summer Inst. in Surface Sci., Milwaukee, 1977, CRC Critical Rev. Solid State Mater. Sci. 7 (1978) 261.

[2] T.B. Grimley, Proc. Phys. Soc. (London) 90 (1967) 751; 92 (1967) 776; J. Am. Chem. Soc. 90 (1968) 3016;
T.B. Grimley and S.M. Walker, Surface Sci. 14 (1969) 395.

[3] T.B. Grimley and M. Torrini, J. Phys. Chem. 6 (1973) 868;
T.B. Grimley, Ber. Bunsenges. Physik. Chem. 75 (1971) 1003.

[4] T.L. Einstein and J.R. Schrieffer, Phys. Rev. B7 (1973) 3629;
T.L. Einstein, Ph.D. thesis, University of Pennsylvania 1973.

[5] N.R. Burke, Surface Sci. 58 (1976) 349.

[6] K.-H. Lau and W. Kohn, Surface Sci. 75 (1978) 69;
T.L. Einstein, Surface Sci. 75 (1978) 161L.

[7] In the case of an alkali on a free-electron-like substrate, the adsorption mechanism is predominantly charge transfer with subsequent electrostatic attraction. The dominant interadatom interaction is then an isotropic dipole–dipole repulsion; no low-coverage islands will form.

[8] T.T. Tsong, Phys. Rev. B6 (1972) 417; 7 (1973) 4018; Phys. Rev. Letters 31 (1973) 1207;
T.T. Tsong, P. Cowan and G. Kellogg, Thin Solid Films 25 (1975) 97;
W.R. Graham and G. Ehrlich, J. Phys. F4 (1974) L212;
D.W. Bassett, Surface Sci. 53 (1975) 74;
D.R. Tice, Surface Sci. 40 (1973) 499.

[9] Even in the grooved case, only nearest and next-nearest neighbors have been extracted to date. K. Stolt, J. Wrigley and G. Ehrlich, in: Proc. 38th Ann. Conf. on Physical Electronics, Oak Ridge, 1978. Moreover, many systems of interest are not presently accessible by FIM.

[10] P.J. Estrup, in: The Structure and Chemistry of Solid Surfaces, Ed. G.A. Somorjai (Wiley, New York, 1969) paper 19.

[11] G. Doyen, G. Ertl and M. Plancher, J. Chem. Phys. 62 (1975) 2957.

[12] W.-Y. Ching, D. Huber, M. Fishkis and M.G. Lagally, J. Vacuum Sci. Technol. 15 (1978) 653;
E.D. Williams, S.L. Cunningham and W.H. Weinberg, J. Chem. Phys. 68 (1978) 4688.

[13] J.C. Buchholz and M.G. Lagally, Phys. Rev. Letters 35 (1975) 442.
[14] G.-C. Wang, T.-M. Lu and M.G. Lagally, J. Chem. Phys., submitted;
M.G. Lagally, G.-C. Wang and T.-M. Lu, invited paper at 3rd Intern. Summer Inst. in Surface Sci., Milwaukee, 1977; CRC Critical Rev. Solid State Mater. Sci. 7 (1978) 233.
[15] M.E. Fisher, Physics 3 (1967) 255;
J. Frenkel, J. Chem. Phys. 7 (1939) 200, 538;
J. Frenkel, Kinetic Theory of Liquids (Oxford Univ. Press, 1946) ch. 7;
W. Band, J. Chem. Phys. 7 (1939) 324, 927;
A. Bijl, Discontinuities in the Energy and Specific Heat, Ph.D. Dissertation, Leiden (1938).
[16] C. Herring, in: Structure and Properties of Solid Surfaces, Eds. R. Gomer and C.S. Smith (Univ. of Chicago Press, Chicago, 1953) p. 5;
C. Herring, Phys. Rev. 82 (1951) 87.
[17] This is a well-known result for the ferromagnetic Ising model. C. Domb, seminar, University of Maryland, Dec. 1975.
[18] In fact, this corresponds to a classic unsolved problem of number theory.
[19] We can derive this result as follows: The only adatom sites that have missing bonds lie within an annulus with width d and the perimeter of the circle as its outer side. Draw a small circle of radius d about an adatom in the annulus; on average the number of missing bonds for this site is twice (or more generally half the number of neighbors d away) the fraction of the circumference of the small circle which lies outside the large circle. The fraction in question, from geometric construction, is $2\theta/2\pi$ where $\cos\theta$ is $(2nx - x^2 - d^2)/(2(n-x)d) \sim x/d$. To get the number of missing bonds this fraction must be integrated over the annulus. In the asymptotic limit, the answer is the factor of 2 times $2nd\sqrt{\pi}$ (the area of the annulus) times π^{-1} (the average of $\cos^{-1}(x/d)/\pi$ over the range 0 to d).
[20] M. von Laue, Z. Krist. 105 (1943) 124.
[21] W.K. Burton, N. Cabrera and F.C. Frank, Phil. Trans. Roy. Soc. (London) 243 (1951) 299.
[22] To construct a "Wulff plot", one marks on a polar graph the free energy per unit length of a flat edge versus the angle of the normal to that edge. One next draws a vector from the origin to each point of the curve and constructs a perpendicular to the radial at the intersection with the curve. The envelope of these perpendiculars is similar to the equilibrium shape of the island [21]. In the case of highly directional bond-type interactions such as considered here, the Wulff plot has inward pointing cusps in the bond directions [16]; perpendiculars to the cusps give the stable shape of the island.
[23] For the sake of comparison, we note that to lowest order, a regular octagon containing n^2 sites has a side of length $[2(1+\sqrt{2})]^{-1/2}n$ and is missing $2.197n$ W_2 bonds and $2.46n$ W_3 bonds.
[24] To count lattice points within a circle, H.B. Keller and J.R. Swenson, Math. Comp. 17 (1963) 223, developed an efficient computer algorithm which first inscribes a square within the circle and then traces out a remaining segment. We have modified the program to calculate the relevant bonds as well.
[25] The absence of a half-monolayer ordered phase corresponds to the well-known absence of an ordered phase in the zero-field triangular Ising antiferromagnetic. G.H. Wannier, Phys. Rev. 79 (1950) 357.
[26] Asymptotically, the (envelope of the) pair interaction decays as R^{-5}, where R is the lateral adatom separation. For small R, the decay is often more precipitous. Cf. refs. [1,2,4,6]. Note $3^{-5/2}$ is 0.0642 while $2^{-5/2}$ is 0.176.
[27] A hexagonal island contains $3m(m+1)+1 \sim 3m^2$ sites, where m is any (positive) integer. For a (2×2) pattern there are $(6m+3)$ missing (attractive) W_3 pairs and $(12m+3)$ W_6 bonds. To order m, for a circle containing this number of sites there are $6(2\sqrt{3}/\pi)^{1/2}$ m missing W_3 bonds and $6(6\sqrt{3}/\pi)^{1/2}$ m missing W_6 pairs.

[28] In terms of Wulff plots entropy effects weaken the cusps (i.e., push them out towards the petals). In three dimensions, this effect is linear in orientation, just like the energy, so that the stronger cusps are simply reduced while some weaker ones are eliminated. In two dimensions, the dependence is logarithmic, eliminating the cusps entirely [16].
[29] Chungpeng Fan and F.Y. Wu, Phys. Rev. 179 (1969) 560. For $W_1 > |W_2|$ the value of T_c is claimed to be accurate to within a few percent.
[30] Work is under way on such faces by P.E. Hunter and T.L. Einstein. If pair interactions depended solely on interadatom separation, then for fcc crystals W_1 would be identical on (100) and (111) faces as would W_3; the W_2 separation on the (111) face is $\sqrt{3}/2 \sim 1.23$ times that on the (100) face.
[31] C.E. Campbell and M. Schick, Phys. Rev. A5 (1972) 1919.
[32] B. Mihura and D.P. Landau, Phys. Rev. Letters 38 (1977) 977.
[33] In the Bethe–Peierls approximation the nearest neighbor Ising model $kT_c/|W_1| = 2/\ln[z/(z-2)]$, where z is the coordination number. See e.g., K. Huang, Statistical Mechanics (Wiley, New York, 1963) ch. 16.
[34] While the phase transition of the (2 × 2) adlayer on a triangular lattice is describable by a 4-state Potts model (R.B. Potts, Proc. Cambridge Phil. Soc. 48 (1952) 106; T. Kihara, Y. Midzuno and T. Shizume, J. Phys. Soc. Japan 9 (1954) 681; S. Alexander, Phys. Letters 54A (1975) 353; E. Domany, M. Schick and J.S. Walker, Phys. Rev. Letters 38 (1977) 1148), this model does not seem helpful in discussing island shapes: the four states correspond to the four possible domains, the interference of which is important for the long-wavelength fluctuations which dominate in the critical region. The shapes of small islands are governed by shorter-range intraisland effects rather than interaction between islands.
[35] T.L. Einstein, Phys. Rev. B16 (1977) 3411.
[36] This issue was carefully discussed in refs. [1] and [35]. The most compelling work indicating the insignificant role of correlation in pair interactions – in sharp contrast to single atom adsorption – is K. Schönhammer, V. Hartung and W. Brenig, Z. Physik B22 (1975) 143.
[37] J.C. Tracy and J.M. Blakely, Surface Sci. 15 (1969) 257;
J.C. Tracy and J.M. Blakely, in: The Structure and Chemistry of Solid Surfaces, Ed. G.A. Somorjai (Wiley, New York, 1969) paper 65.
[38] See, e.g., B. Rossi, Optics (Addison-Wesley, Reading, MA, 1957) p. 208 (fig. 4-50).
[39] J.E. Houston and R.L. Park, Surface Sci. 21 (1970) 209, consider the opposite case of dence abuting islands, in which only the extra spots carry adlayer information.
[40] On the integer-order LEED spots, the stars are usually masked by the scattering intensity from the substrate atoms, which are more numerous and typically higher-Z than the adatoms.
[41] L.D. Roelofs and T.L. Einstein, unpublished.
[42] A. Sommerfeld, Optics (Academic Press, New York, 1954) p. 234.
[43] M.B. Webb and M.G. Lagally, Solid State Phys. 28 (1973) 301.
[44] R.L. Park, J.E. Houston and D.G. Schreiner, Rev. Sci. Instr. 42 (1971) 60.
[45] L.D. Roelofs, R.L. Park and T.L. Einstein, J. Vacuum Sci. Technol. 16 (1979).
Because of the precise relationship, the width of the Fourier transform of the transfer function, gauged by the square root of its second moment, is $\sqrt{2}$ times the width of the corresponding window function. In quantitative studies, the detailed form of these functions may all play some subtle role.
[46] R.L. Park, J. Appl. Phys. 37 (1966) 295;
R.L. Park, in: The Structure and Chemistry of Solid Surfaces, Ed. G.A. Somorjai (Wiley, New York, 1969) paper 28;
R.L. Park and J.E. Houston, Surface Sci. 18 (1969) 213.

[47] T.-M. Lu, G.-C. Wang and M.G. Lagally, Phys. Rev. Letters 39 (1977) 411.
[48] G.-C. Wang and M.G. Lagally, private communications;
G.-C. Wang, in : Proc. 38th Ann. Conf. on Physical Electronics, Oak Ridge, 1978;
G.-C. Wang, Ph.D. dissertation, Univ. of Wisconsin, Madison (1978, unpublished).
[49] See, e.g., K. Binder and H. Müller-Krumbhaar, Phys. Rev. B9 (1974) 2328;
K. Binder, D. Stauffer, and H. Müller-Krumbhaar, Phys. Rev. B12 (1975) 5261.
[50] K. Binder and D. Stauffer, J. Statistical Phys. 6 (1972) 49. They found that island size varies as perimeter squared only when the diameter exceeds the critical-phenomena coherence length, but this length is small at the temperatures envisioned in our problem.
[51] L.D. Roelofs, private communication; cf. ref. [45].
[52] Reviews include R. Gomer, Solid State Phys. 30 (1975) 93 (esp. 115–121): CRC Rev. Solid State Sci. 7 (1978) 119; H.P. Bonzel, CRC Critical Rev. Solid State Sci. 6 (1976) 171.
[53] A.R. Kortan has painstakingly sorted through the vast literature on adsorption systems. Except for recent studies, most references are given by G.A. Somorjai and F.J. Szalkowski; J. Chem. Phys. 54 (1971) 389; G.A. Somorjai and L.L. Kesmodel, in MTP Review on Surface Science, Ed. M. Kerker (Butterworth, London, 1974).
[54] M.R. Leggett and R.A. Armstrong, Surface Sci. 24 (1971) 404.
[55] K. Yonehara and L.D. Schmidt, Surface Sci. 25 (1971) 238;
T.E. Felter, R.A. Barker and P.J. Estrup, Phys. Rev. Letters 38 (1977) 1138;
M.K. Debe and D.A. King, J. Phys. C10 (1977) L303; Phys. Rev. Letters 39 (1977) 708;
R.A. Barker, P.J. Estrup, F. Jona and P.M. Marcus, Solid State Commun. 25 (1978) 375.
[56] R.A. Barker and P.J. Estrup, Phys. Rev. Letters 41 (1978) 1307.
[57] A.U. MacRae, Surface Sci. 1 (1964) 319.
[58] P.H. Holloway and J.B. Hudson, Surface Sci. 43 (1974) 141.
[59] T.E. Madey, H.A. Engelhardt and D. Menzel, Surface Sci. 48 (1975) 304.
[60] A.R. Kortan, M.L. DenBoer and R.L. Park, in: Proc. 38th Ann. Conf. on Physical Electronics, Oak Ridge, 1978;
A.R. Kortan, P.I. Cohen and R.L. Park, J. Vacuum Sci. Technol., to be published.
Unfortunately, even for O/Ni the oxygen is not confined to the surface at all coverages.
See also:
R.L. Park and H.E. Farnsworth, Appl. Phys. Letters 3 (1963) 167; J. Appl. Phys. 35 (1964) 2220;
E.I. Alessandrini and J.R. Freedman, Acta Cryst. 16 (1963) 54.